

Research Article

FORTUNE JOURNAL OF HEALTH SCIENCES

ISSN: 2644-2906



Extracellular Thioredoxin, not its Intracellular Counterpart, Mediates Homocysteine Thiolactone- Induced Vascular Endothelial Cell Dysfunction

Ping Liu and Liangwei Zhong*

Abstract

Background: Our previous work demonstrated an inverse correlation between serum total homocysteine (Hcy) levels and thioredoxin (Trx) activity in patients with coronary artery stenosis. However, whether homocysteine thiolactone (HCTL), a highly reactive Hcy derivative, affects Trx remains unknown.

Methods: Using human cytosolic thioredoxin (hTrx1) as a model, we employed a multidisciplinary approach—integrating biochemical assays, mass spectrometry, electron microscopy, and vascular endothelial cell models—to investigate HCTL-induced regulation. We systematically examined the effects of HCTL exposure (0–250 μ M) on hTrx1 structure and function, both intracellularly and extracellularly.

Key Findings: Hcy-hTrx1 complexes were present in human serum. While increasing extracellular HCTL elevated cellular levels of Hcy and Hcy-hTrx1 complexes, these changes did not compromise vascular endothelial cell viability. However, HCTL covalently modified extracellular hTrx1 at Lys36 and Lys39, forming *N*-homocysteinylated hTrx1 (*N*-Hcy-hTrx1). This modification severely impaired hTrx1's activity and properties, triggered amyloid-like fibril formation, and exhibited marked cytotoxicity—667-fold higher than HCTL alone. Additionally, we detected serum autoantibodies specific to *N*-Hcy-hTrx1.

Conclusions: Extracellular *N*-Hcy-hTrx1, not free HCTL or intracellular hTrx1, serves as the primary cytotoxic mediator. The presence of serum auto-antibodies specifically targeting *N*-Hcy-hTrx1 further supports its pathogenic role *in vivo*. This study reveals a novel mechanism through which extracellular hTrx1 connects hyperhomocysteinemia to vascular endothelial cell dysfunction.

Keywords: Cardiovascular disease; Homocysteine; Homocysteine thiolactone; *N*-Homocysteinylation; Protein aggregation; Protein chemical modification; Thioredoxin

Introduction

Patients with coronary artery disease (CAD) frequently exhibit elevated plasma/serum levels of total homocysteine (tHcy) [1] alongside reduced thioredoxin activity [2,3], yet the molecular mechanisms underlying this inverse relationship remain poorly understood. tHcy consists of free thiol-containing homocysteine (HcySH) and oxidized forms, including homocystine (Hcy-S-S-Hcy) and mixed disulfides (Hcy-S-S-Cys or Hcy-S-S-protein) [4]. During protein-associated homocysteine (Hcy) metabolism, homocysteine thiolactone (HCTL) is generated [5], with elevated levels observed in hyperhomocysteinemia

Affiliation:

Medical School, University of Chinese Academy of Sciences, the Campus of Yanqi, Huai Rou, 101407 Beijing, China

*Corresponding author: Prof. Liangwei Zhong, Ph.D

E-mail: liazho@ucas.ac.cn

Citation: Ping Liu, Liangwei Zhong, Extracellular Thioredoxin, not its Intracellular Counterpart, Mediates Homocysteine Thiolactone-Induced Vascular Endothelial Cell Dysfunction. Fortune Journal of Health Sciences. 8 (2025): 1077-1088.

Received: October 15, 2025 Accepted: October 22, 2025 Published: November 13, 2025



[6]. Since cellular HCTL synthesis correlates directly with HcvSH concentrations [6,7], its role in CAD pathogenesis warrants further investigation. HCTL is a highly reactive intramolecular thioester [8], that readily diffuses across membranes due to its neutral charge at physiological pH, allowing its detection in human plasma/serum and cell culture media [6]. Notably, HCTL preferentially modifies Lys residues in proteins via ε-amino group adduction, forming N-linked homocysteinylated proteins (9). This modification, termed protein N-homocysteinylation, occurs even at low HCTL concentrations (≥10 nmol/L) [10] and can induce protein misfolding, amyloid-like aggregation [11,12], and vascular dysfunction [13,14]. Given these effects, N-homocysteinylation may contribute to CAD progression, but the role of hTrx1 as a target remains poorly characterized. Thioredoxin (Trx), a key antioxidant protein, plays critical roles in cardiovascular homeostasis [15-17]. Human cytosolic thioredoxin (hTrx1) localizes to the cytosol, nucleus [18] and extracellular space [3], where it regulates diverse processes, including cell survival [16,19], insulin signaling [20] [21] and inflammatory responses [22,23]. The functional integrity of hTrx1 depends on its redox-active site Cys residues (Cys32 and Cys35) as well as structural Cys residues (Cys62, Cys69, and Cys73), which are susceptible to post-translational modifications [24-26]. However, whether hTrx1 is a target of N-homocysteinylation, and how such modification affects

its function have not been exploring. Given hTrx1's twelve Lys residues, we hypothesized that HCTL could modify them to generate N-homocysteinylated hTrx1 (N-HcyhTrx1). Here, we demonstrate the formation of N-Hcy-hTrx1 both in vitro and in vivo. Surprisingly, extracellular N-HcyhTrx1 aggregates into fibrillar structures and exhibits ~667fold greater cytotoxicity than HCTL alone. Although HCTL exposure leads to cellular Hcy-hTrx1 complex formation, alters hTrx1 activity, and induces fluctuations in redox states, these changes do not affect endothelial cell viability. Instead, our findings reveal that extracellular N-Hcy-hTrx1, rather than intracellular redox alterations, serves as a major driver of vascular cytotoxicity. These results redefine the mechanistic understanding of HCTL toxicity and highlight a novel pathway by which high Hcy/HCTL levels contribute to CAD pathogenesis.

Results

hTrx1 is a target of Hcy modification in the human body

Serum hTrx1, a cytosolic protein that can be secreted into the circulation, exhibits an inverse correlation between its activity and total homocysteine (tHcy) levels in human serum [2]. However, the mechanism underlying this relationship remains unclear. To determine whether Hcy directly interacts

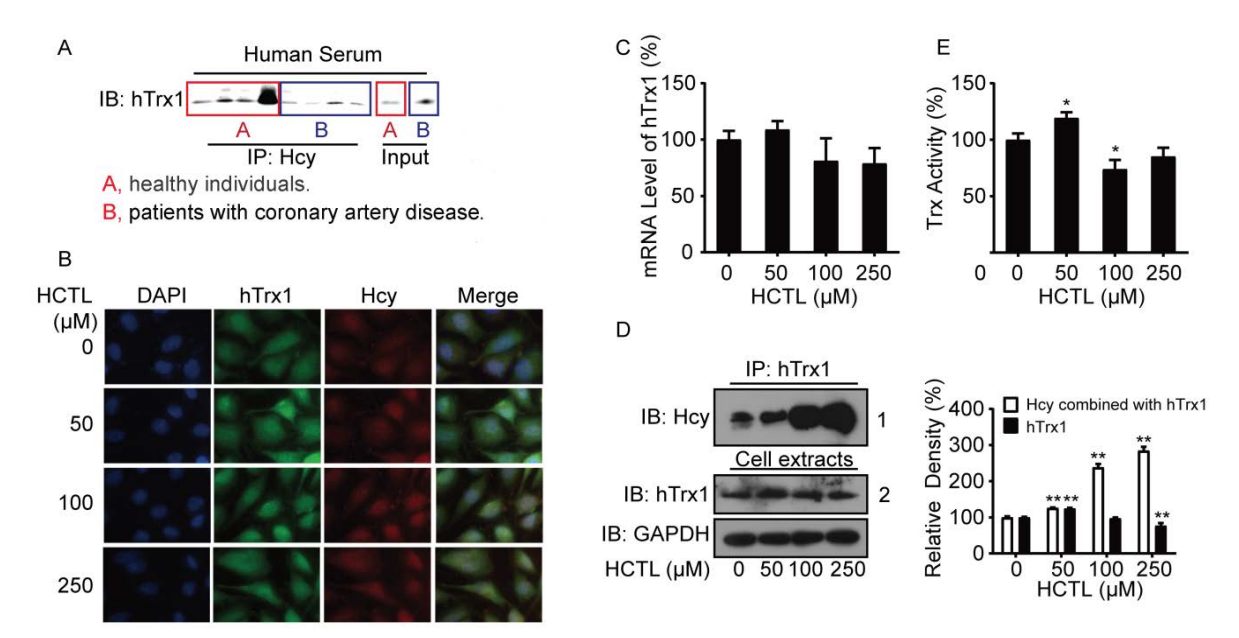


Figure 1: Association of Hcy/HCTL with hTrx1. (A) Immunoprecipitation. Proteins immunoprecipitated (IP) from human serum using an anti-Hcy antibody were analyzed by Western blot (Immunoblotting, IB) with an anti-hTrx1 antibody. "Input" represents the total serum protein prior to immunoprecipitation. (B) Immunofluorescence staining was performed on cells using antibodies against anti-hTrx1 (green) and anti-Hcy (red). (C) Quantitative Real-Time PCR analysis of hTrx1 mRNA expression, normalized to β-actin. Data are represented as the mean \pm SD (n=3). (D) *Left panel*: Immunoblot analysis of homocysteinylated hTrx1. Cell extracts were immunoprecipitated (IP) using an anti-hTrx1 monoclonal antibody, followed by immunoblotting (IB) with the indicated antibodies. *Right panel*: Quantification of band intensities from three independent experiments (mean \pm SD). **P < 0.01 vs. HCTL-untreated control. (E) Trx activity in cell extracts, expressed as a percentage of the control (mean \pm SD; n≥3). *P < 0.05 vs. HCTL-untreated control.



with hTrx1 *in vivo*, we immunoprecipitated (IP) Hcy-bound proteins from human serum using an anti-Hcy polyclonal antibody. Subsequent Western blot analysis with an anti-hTrx1 monoclonal antibody confirmed the presence of hTrx1 in the Hcy-bound protein complex (Fig. 1A), indicating that hTrx1 is a target of Hcy modification in the human body.

Impact of extracellular HCTL on hTrx1 localization, expression, and activity

Since HCTL passively diffuses across cell membranes once accumulation in culture media [7], we treated human vascular endothelial cells with exogenous HCTL to evaluate its effects on cellular hTrx1. Using double immunofluorescent staining, we analyzed the subcellular distribution of Hcy and hTrx1. In untreated cells (0 µM HCTL), both Hcy and hTrx1 were predominantly localized in the cytoplasm. Treatment with 50 μM HCTL increased intracellular levels of Hcy and hTrx1, with notable nuclear accumulation. At 100 μM HCTL, Hcy levels further increased, particularly in the nucleus, alongside enhanced co-localization with nuclear hTrx1. Exposure to 250 µM HCTL resulted in complete co-localization of Hcy and hTrx1 throughout the cell (Fig. 1B). Next, we evaluated how extracellular HCTL influences hTrx1 expression. While 50 µM HCTL slightly elevated hTrx1 mRNA levels, concentrations ≥100 µM reduced hTrx1 mRNA, though these changes were not statistically significant (Fig. 1C). Notably, 50 μM HCTL significantly increased total thioredoxin (Trx) activity (which detects both cytoplasmic and mitochondrial Trx), whereas 100 µM and 250 µM HCTL suppressed it (Fig. 1E). This biphasic response aligned with trends in hTrx1

mRNA (Fig. 1C) and protein levels (Fig. 1D, right panel).

In summary, 50 μ M HCTL enhanced hTrx1 expression and activity, whereas higher concentrations ($\geq 100~\mu$ M) exerted inhibitory effects. However, the formation of the Hcy-hTrx1 complex increased proportionally with extracellular HCTL levels (Fig. 1D, the first line in the left panel). Importantly, Hcy binding to hTrx1 intensified at higher HCTL concentrations (Fig. 1D), irrespective of whether hTrx1 protein levels increased or decreased (Fig. 1D, the second line in the left panel).

Effects of extracellular HCTL on cellular hTrx1 redox states, ROS levels, and cell viability

The functional diversity of hTrx1 is closely tied to the redox states of its thiol groups, which can adopt different forms in cells. To assess how HCTL influences intracellular hTrx1 redox status, we performed an electrophoretic redox Western blot [27]. Under physiological conditions, free thiols in hTrx1 were alkylated with iodoacetic acid (IAA), introducing negative charges at pH 8.0 and causing faster electrophoretic migration compared to uncharged thiols modified by iodoacetamide (IAM). This charge-based separation of IAA-alkylated hTrx1 isoforms allowed quantification of the initial free thiol content [28], with the mobility standard prepared as previously described [28]. We found that cellular hTrx1 predominantly existed in three isoforms, each with 2, 3, or 4 thiol groups, regardless of whether the culture medium contains 50 µM HCTL. However, treatment with higher HCTL concentrations (100 or 250 µM) reduced the

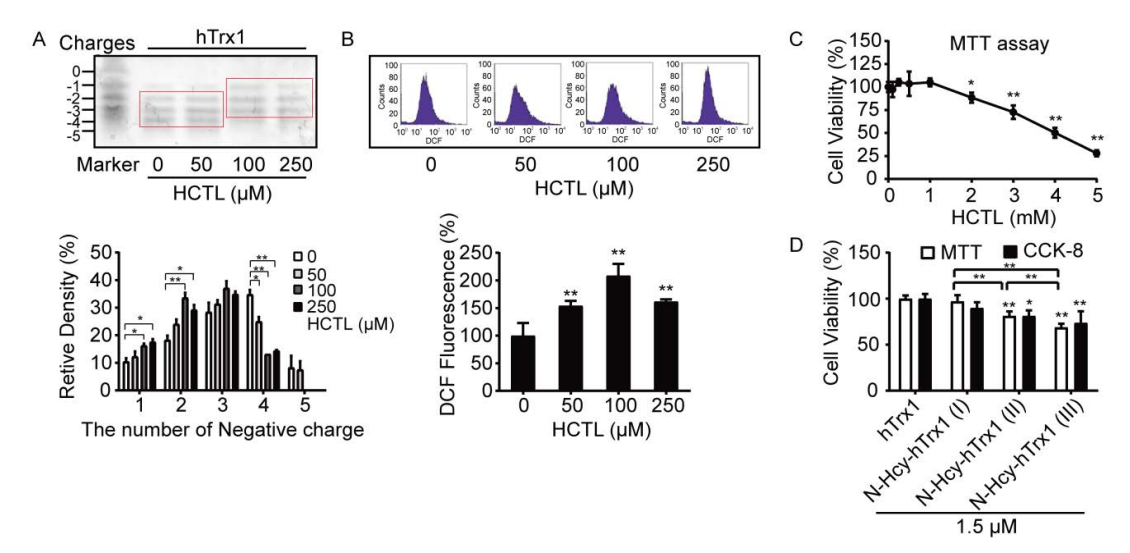


Figure 2: Effects of extracellular HCTL on hTrx1 thiol status, ROS levels, and cell viability. (A) Redox state of hTrx1. (*Upper panel*) Redox Western blot of hTrx1. (*Lower panel*) Densitometric analysis of Western blot bands. Relative band densities were normalized to untreated controls. Data represent mean \pm SD from three independent experiments. P < 0.05; **, P < 0.01. (B) Cellular ROS levels. (*Upper panel*) Representative flow cytometry histogram. (*Lower panel*) Quantification of ROS levels. Data are mean \pm SD of three independent experiments. **, P < 0.01 vs. untreated control. (C) Cell viability assessed by MTT assay. Data points represent mean \pm SD from six independent experiments. *, P < 0.05; **, P < 0.01 vs. untreated control. (D) Comparison of MTT and CCK-8 assays. Control cells were treated with buffers instead of enzyme solution. Data represent mean \pm SD from six independent experiments. *, P < 0.05; **, P < 0.01 vs. control (connecting lines omitted).



accessibility of thiols to IAA, increasing the proportion of the single-thiol isoform while decreasing the four-thiol isoform (Fig. 2A). Moreover, exposure to extracellular HCTL (50–250 μ M) resulted in a 0.5 to 2-fold increase in intracellular ROS levels (Fig. 2B). None of these changes affected cell viability (Fig. 2C).

N-homocysteinylation at specific Lys residues in hTrx1 mediated cytotoxicity toward vascular endothelial cells

In contrast, cell viability was significantly reduced by treatment with 1.5 µM N-Hcy-hTrx1(I), N- Hcy-hTrx1(II), or N-Hcy-hTrx1(III) (Fig. 2D). Notably, N-Hcy-hTrx1 exhibited greater cytotoxicity toward vascular endothelial cells than HCTL alone. To elucidate the underlying mechanism, we analyzed the binding sites of HCTL on N-Hcy-hTrx1(III) using LC-ESI-MS/MS. Peptide coverage spanned 60% of the N-Hcy-hTrx1(III) sequence, including a peptide containing the active-site "Cys-X-X-Cys" motif (Fig. 3A). Among the y-type fragment ions, the observed y4 ion $(384.82 \times 2 \text{ Da})$ showed a 249.76 Da increase compared to the theoretical mass (519.88 Da). This mass shift corresponds to the addition of two N-homocysteinyl moieties (N-Lys-Hcy-SH, 117 Da each [39] at Lys36 and Lys39, along with oxidation (+15.99 Da) of Met37. Further confirmation came from mass differences between y16++ and y21++, which matched theoretical predictions and ruled out modification at Lys21. A series of b-type fragment ions (b13 to b23) further excluded N-homocysteinylation at Lys21. Collectively, these results demonstrate that N-homocysteinylations selectively target Lys36 and Lys39, which flank the active-site Cys35 (Fig. 3A, insert a). To determine whether elevated HCTL levels increase N-Hcy-hTrx1 formation, we incubated hTrx1 with increasing HCTL concentrations (0, 5, 10, 25, 50, or 100-fold molar excess) for 24 h and then labeled free thiols with the fluorescent dye 5-IAF. Fluorescence intensity increased proportionally with HCTL concentration, reflecting the incorporation of new thiol groups via N-homocysteinylation. Saturation was observed at a 50:1 molar ratio of HCTL to hTrx1 (Fig. 3A, panel b), confirming that N-homocysteinylation modifies specific Lys residues rather than all available sites.

N-Homocysteinylation of hTrx1 induces aggregation and auto-antibody recognition

N-Hcy-hTrx1(III) readily formed precipitates, which contained high-molecular-weight complexes (red box, lane 3, Fig. 3B). These aggregates were partially dissolved by treatment with 100 mM DTT (lane 4, Fig. 3B), indicating that disulfide bonds contribute to—but are not solely responsible for—their stabilization. In contrast, N-Hcy-hTrx1(I) did not form significant precipitates (lane 2, Fig. 3B). Although both N-Hcy-hTrx1(I) and N-Hcy-hTrx1(III) exhibited significantly lower activity than native hTrx1, their activities did not differ substantially from each other (Fig. 3C).

N-Homocysteinylation is known to induce structural alterations in proteins, potentially generating neo-self antigens. Indeed, anti-N-Hcy-protein autoantibodies have been identified in human serum [29]. To evaluate IgG binding specificity to N-Hcy-hTrx1, we performed dot-blot analysis using human sera as primary antibodies. A representative serum reaction (Fig. 3D) revealed stronger binding to N-Hcy-hTrx1(I) than to native hTrx1, supporting the hypothesis that N-Hcy-hTrx1 formation triggers autoantibody production in vivo.

N-Homocysteinylation induced structural and functional alterations in hTrx1 leading to amyloid-like aggregation

- (i) Proteolytic resistance. Proteinase K, a broadspectrum protease, efficiently degrades a wide range of proteins, including those resistant to other proteases. After incubation with proteinase K, native hTrx1 was gradually digested into small fragments, whereas *N*-Hcy-hTrx1(III) remained resistant to degradation (Fig. 3E), suggesting either structural stabilization or inaccessibility of cleavage sites due to *N*-homocysteinylation.
- (ii) Secondary structural changes revealed by CD spectroscopy. CD spectroscopy demonstrated distinct secondary structural differences between native and N-Hcy-hTrx1. Native hTrx1 exhibits a characteristic spectrum with a negative peak at 220 nm (α -helices) and a positive peak at 194 nm (β -sheets) (Line 1, Fig. 4A), consistent with its known structure (four α -helices and five β -sheets) [30,31]. In contrast, N-Hcy-hTrx1(I) and (III) displayed reduced α -helical content (Lines 2 and 3, Fig. 4A), indicating substantial conformational rearrangements.
- (iii) Fluorescence quenching indicated changes in microenvironment. hTrx1 contains a single Trp31 residue near the active site "-Cys32-X-X-Cys35-" motif and a single Tyr49 residue adjacent to Lys48 (Insert a, Fig. 3A). Native hTrx1 exhibited emission maxima at 334 nm (Trp31) and 310 nm (Tyr49) (Fig. 4B, left panel) (32,33). Upon N-homocysteinylation, fluorescence intensity decreased progressively: N-Hcy-hTrx1(I) (10-fold HCTL excess, 8 h) showed 28.7% decrease at 334 nm, 12.9% decrease at 310 nm; N-Hcy-hTrx1(III) (100-fold HCTL excess, 8 h) exhibited additional 5.5% decrease at 334 nm. Extended incubation (24 h) further reduced fluorescence intensity (42.8–55.9% at 334 nm, 20.9-34.7% at 310 nm) (Fig. 4B, right panel). Since Lys48 remained unmodified, the fluorescence quenching likely results from N-homocysteinylation of Lys36/39, which reduces solvent exposure of Trp31 and Tyr49. Given that Trp31 is critical for hTrx1 function [34], these modifications likely impair activity.



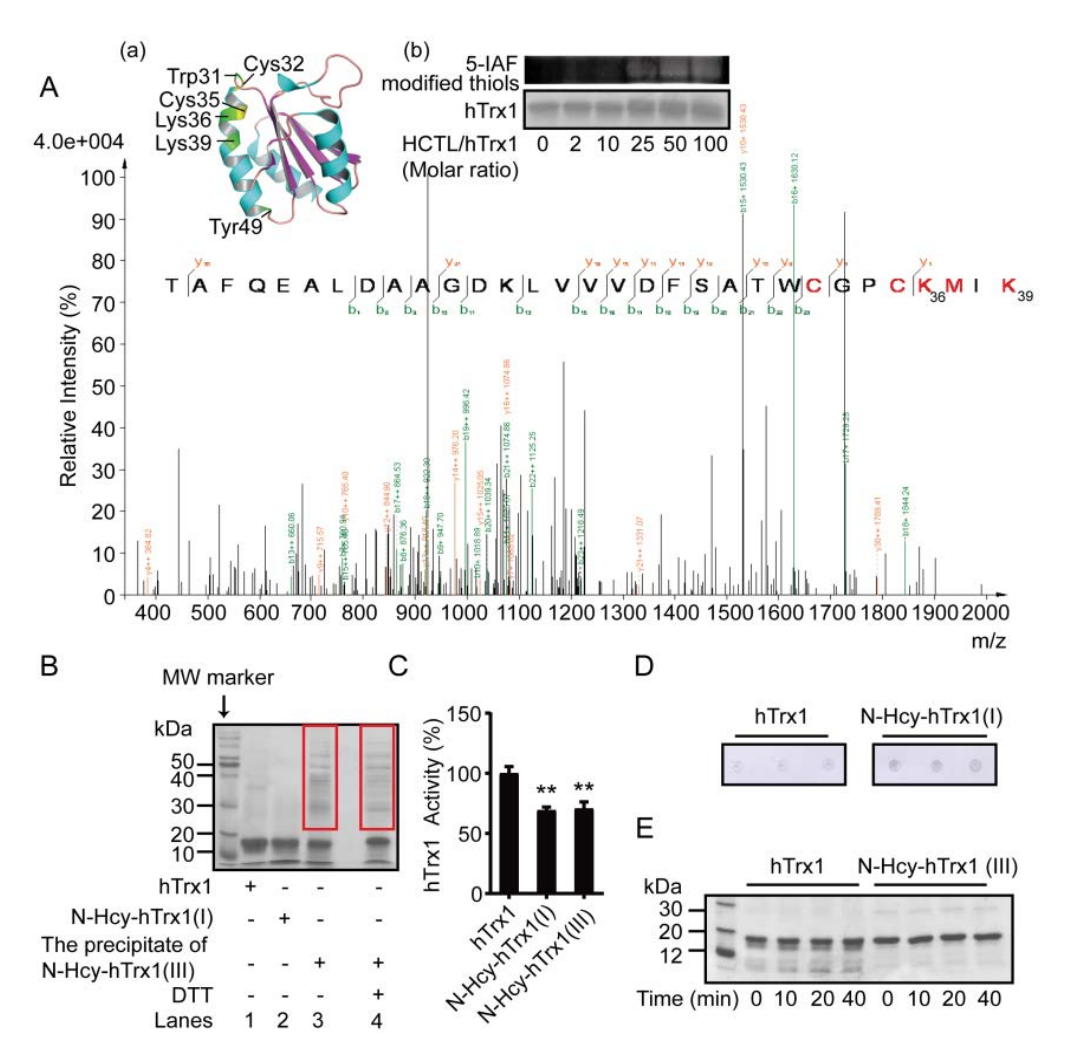


Figure 3: Properties of N-homocysteinylated hTrx1. (A) Identification of HCTL-modified Lys residues by LC-ESI-MS/MS. (Inset a) Distribution of Lys36 and Lys39 on the tertiary structure of hTrx1 (PDB: 5DQY). (Inset b) (Panel 1) N-homocysteinylated Trx1 was incubated with 5-IAF, separated by SDS-PAGE, and detected by fluorescence (upper) or Coomassie Brilliant Blue staining (lower). (Panel 2) Relative fluorescence intensity. (B) SDS-PAGE analysis of hTrx1 after 24 h incubation with HCTL. (C) Insulin reduction assay. Data represent mean \pm SD of three independent experiments. **P < 0.01 ν s. hTrx1. (D) Dot blot probed with human serum as the primary antibody. (E) SDS-PAGE of samples after proteinase K digestion.

Increased hydrophobicity and amyloid-like properties. To assess changes in hydrophobicity, we utilized ANS fluorescence. ANS is not inherently fluorescent in an aqueous environment; however, it exhibits high fluorescence upon binding to the solvent-exposed hydrophobic regions of proteins, accompanied by a blue shift in the emission λmax [35]. While native hTrx1 and N-Hcy-hTrx1(I) showed minimal ANS binding, N-Hcy-hTrx1(III) exhibited a strong increase in fluorescence intensity and a blue shift (Fig. 4C), indicating exposed hydrophobic patches that may drive aggregation. Thioflavin T (ThT) binding, a hallmark of amyloid-like structures [36], was significantly enhanced in N-Hcy-hTrx1(III) but absent in native hTrx1 and N-HcyhTrx1(I) (Fig. 4D), suggesting that N-Hcy-hTrx1(III) possesses β-sheet-rich amyloidogenic properties.

(v) Morphological evidence of aggregation. Microscopy revealed striking morphological differences: Native hTrx1 + ThT showed no fluorescence or aggregates (Fig. 4E, panels a & c); *N*-Hcy-hTrx1(II) + ThT displayed fluorescent aggregates visible under both fluorescence and DIC microscopy (Fig. 4E, panels b & d). TEM imaging further confirmed structural changes: native hTrx1 appeared as homogeneous spheres, whereas *N*-Hcy-hTrx1(II) formed fibrillar structures (Fig. 4F).

Discussion

The differing responses of intra- and extracellular hTrx1 to HCTL.

Human serum contains autoantibodies targeting N-Hcy-hTrx1, providing critical evidence for its presence *in vivo*



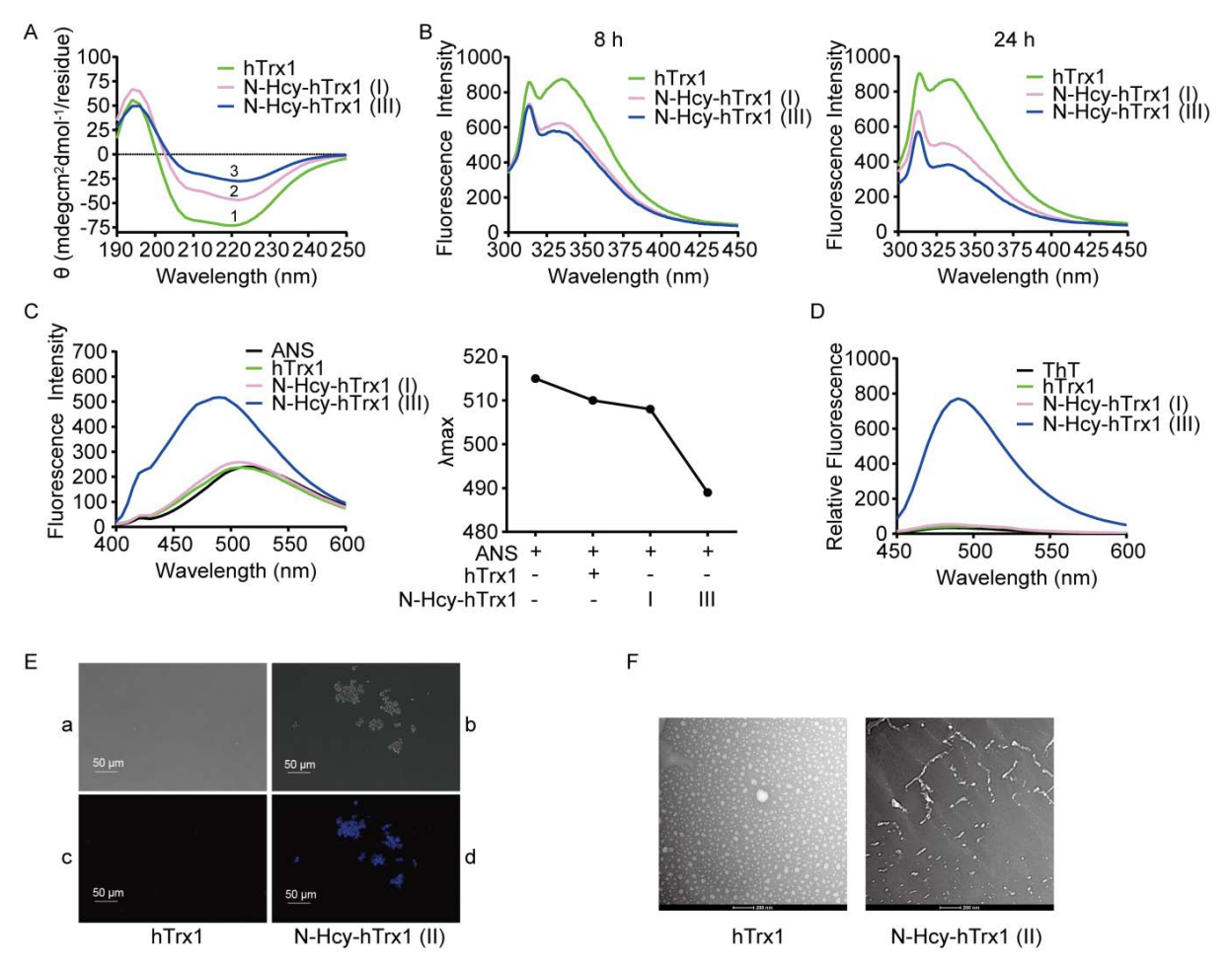


Figure 4: Structural changes in hTrx1 induced by *N*-homocysteinylation. (**A**) Circular dichroism (CD) spectra. Data represent the mean of three independent experiments. Control buffer scans (n = 3) were subtracted from sample spectra. (**B**) Time-dependent changes in intrinsic fluorescence intensity upon *N*-homocysteinylation. (**C**) *N*-homocysteinylation effects on ANS fluorescence. Left: Emission intensity; Right: Blue shift in fluorescence emission maxima. (**D**) Thioflavin T (ThT) fluorescence emission spectra after *N*-homocysteinylation. (**E**) Morphological analysis. hTrx1 (a, c) and *N*-Hcy-hTrx1(II) (b, d) were incubated with ThT and imaged by fluorescence microscopy (a, b) and differential interference contrast (DIC) microscopy (c, d). (**F**) Transmission electron microscopy (TEM) images.

and suggesting a potential role in autoimmune diseases. Autoantibodies are well-established markers of autoimmune conditions [37]. In fact, some autoimmune disorders are linked to an elevated risk of cardiovascular disease [38]. The novel detection of anti-N-Hcy-hTrx1 autoantibodies highlights the need for further investigation into their clinical relevance. The presence of Hcy-hTrx1 complexes in both healthy individuals and those with CAD suggests a sophisticated mechanism for HCTL in modulating hTrx1. The redox state of hTrx1 determines its susceptibility to modification. In the extracellular environment, hTrx1 exists in an oxidized state, lacking free thiol groups, which renders it susceptible to modification by HCTL but not by HSSH/ HcySH. In contrast, intracellular hTrx1 is typically reduced, with available thiol groups for HSSH/HcySH modification. While HCTL could theoretically modify cellular hTrx1,

experimental data suggest otherwise.

Key findings support this distinction: High extracellular HCTL concentrations reduced the thiol content of cellular hTrx1 (Fig. 2A), ruling out *N*-homocysteinylation (which would introduce additional thiol groups). This contrasts with extracellular hTrx1, where HCTL modification raised thiol levels (Fig. 3A, panel B). At 250 μM extracellular HCTL, cellular Hcy-hTrx1 complexes accumulated without cytotoxicity (Fig. 2C), further suggesting these were not *N*-Hcy-hTrx1—a modification known to be highly cytotoxic even at low concentrations (Fig. 2D). The discrepancy likely arises from HCTL degradation into HcySH, which modifies thiol groups to form *S*-Hcy-proteins [39], consistent with the thiol depletion observed in Fig. 2A.



HCTL exhibits concentration-dependent dual regulation of hTrx1 and ROS in vascular endothelial cells

In human vascular endothelial cells, HCTL treatment induced biphasic responses in hTrx1: adaptive response at low levels vs. inhibition at high concentrations. At 50 µM, HCTL increased hTrx1 expression, likely due to a 1.5-fold rise in ROS (Fig. 2B). Since low-level ROS can act as signaling molecules and hTrx1 is known to be upregulated by oxidative stress [40], this may represent an adaptive response to mild oxidative stimuli. In contrast, at concentrations >100 μM, HCTL inhibited hTrx1, suppressing its protein expression and activity while markedly increasing Hcy-hTrx1 complex formation (Fig. 1D). Thus, HCTL appears to modulate hTrx1 through at least two mechanisms: transcriptional regulation and direct protein binding. Notably, extracellular HCTL increased cellular ROS levels by 1.5-fold at 50 and 250 μM, but by 2-fold at 100 μM (Fig. 2B). While 100 and 250 µM HCTL reduced hTrx1 thiol content, 50 µM had no effect (Fig. 2A). This thiol loss may not result solely from oxidation, S-homocysteinylation could also contribute, as HCTL hydrolysis generates protein S-homocysteinylation [39]. Additionally, bleomycin hydrolase, an intracellular enzyme, exhibits Hcy-thiolactonase activity [41], which could further influence these modifications. Under physiological conditions, plasma tHcy levels in healthy individuals remain below 15 µM, with HCTL concentrations ranging from 0 to 34.8 nmol/L (0.002-0.3% of plasma tHcy) [10]. At these levels, HCTL has negligible effects on hTrx1 function, ROS production, and N-Hcy-hTrx1 formation, resulting in significantly less vascular endothelial cellular damage than that observed in hyperhomocysteinemia.

N-homocysteinylation of hTrx1 impairs activity via active-site conformational disruption.

N-Homocysteinylation significantly activity of native hTrx1 (Fig. 3C), likely due to structural perturbations at Lys36 and Lys39. To investigate these changes, we analyzed Trp and Tyr fluorescence, which are sensitive to microenvironment alterations. hTrx1 contains Trp31 (adjacent to the active-site Cys32) and Tyr49 (Fig. 3A, Panel a). While Trp31 fluorescence is highly environmentdependent, Tyr49 exhibits weaker sensitivity. After 8 h of HCTL incubation, both N-Hey-Trx1(I) and N-Hey-Trx1(III) showed a marked decrease in Trp31 emission, with a smaller reduction in Tyr49 fluorescence. The similar decline between the two modified forms suggests comparable active-site conformational changes at this stage. Extending incubation to 24 h further reduced fluorescence, with N-Hcy-Trx1(III) exhibiting a more pronounced decrease than N-Hcy-Trx1(I), indicating that active-site distortion depends on both HCTL concentration and reaction time. These findings align with the observed loss of enzymatic activity in N-homocysteinylated

hTrx1 (Fig. 3C). Notably, Lys36 is critical for hTrx1 function and growth promotion [42]. In the oxidized structure, the carbonyl groups of Cys32 and Gly33 form well-aligned hydrogen bonds with the amide nitrogens of Lys36 and Met37, respectively, in helix α-2 (Fig. 3A, insert a) [34]. These hydrogen bonds are essential for the reversibility of hTrx1 redox cycling. *N*-Homocysteinylation of Lys36 likely disrupts these interactions, further compromising enzymatic function.

N-Homocysteinylation of hTrx1 induces structural changes.

The isoelectric point (pI) of hTrx1, calculated as 4.828 using Prot pi | Protein Tool, is classified as an acidic protein, rendering it particularly susceptible to modification by HCTL [43]. This modification leads to the formation of N-homocysteinylated hTrx1 (N-Hcy-hTrx1) in a HCTL concentration-dependent manner, as demonstrated by the increase in free thiol content (Fig. 3A, insert b). Among the modified species, N-Hcy-hTrx1(I) exhibits minimal structural perturbation, whereas N-Hcy-hTrx1(II) and (III) display a pronounced tendency to aggregate, forming fibrillar structures with reduced enzymatic activity and increased cytotoxicity (Fig. 2D). The structural and functional alterations induced by *N*-homocysteinylation arise from the following key changes: (i) Exposure of Hydrophobic Regions (ANS Fluorescence). Native hTrx1 and N-Hcy-hTrx1(I) display low ANS emission (peak at ~520 nm, similar to free ANS), indicating limited hydrophobic exposure. In contrast, N-Hcy-hTrx1(III) exhibits a strong ANS signal with a blue shift, suggesting exposed hydrophobic patches—a hallmark of protein misfolding and aggregation. (ii) Loss of α-Helical Structure (Far-UV CD Spectroscopy). Native hTrx1 adopts an α/β structure, featuring a central β -sheet flanked by α -helices. Modification of Lys36 and Lys39 disrupts these stabilizing interactions, leading to α-helix destabilization and increased β-sheet formation. (iii) Proteinase K Resistance (Indicative of β-Sheet Enrichment). N-Hcy-hTrx1(III) shows resistance to Proteinase K digestion even after 40 min, implying oligomerization into β-sheet-rich aggregates. This behavior is characteristic of amyloid-like fibrils, which are typically protease-resistant [44].

N-Homocysteinylation drives amyloid formation in hTrx1.

Amyloid structures are secondary structures linked to cytotoxicity during their interaction with the cell membrane [45]. ThT has been widely used to investigate amyloid formation. Upon binding to amyloid fibrils, ThT gives a strong fluorescence [46,47]. N-Hcy-hTrx1(III) showed strong ThT fluorescence at 495 nm, indicating amyloid formation, while native hTrx1 and N-Hcy-hTrx1(I) did not. This suggests that N-Hcy-hTrx1(III) forms amyloid fibrils, which correlates with its higher cytotoxicity (Fig. 2D). N-Hcy-hTrx1(II) also exhibited increased ThT fluorescence (Fig. 4E).



Transmission electron microscopy (TEM) revealed fibrillar structures in N-Hcy-hTrx1(II) (Fig. 4F), confirming amyloid formation. N-Hcy-hTrx1(I), which lacks amyloid structures, showed no cytotoxicity. These results demonstrate that N-homocysteinylation can drive amyloid formation in hTrx1, with structural variants (II and III) being cytotoxic due to fibril formation, while variant (I) remains non-toxic. Apparently, at high HCTL levels, N-Hcy-hTrx1(II)/(III) adopt a β-sheetrich secondary structure, exposing hydrophobic surfaces. This promotes protein aggregation into amyloid fibrils, which can disrupt cell membranes and induce toxicity. The findings highlight the importance of maintaining normal Hcy/ HCTL levels in the body and that high Hcy/HCTL levels can cause protein homocysteinylation, which in turn can induce amyloid formation and cytotoxicity. This mechanism may underlie diseases associated with hyperhomocysteinemia, such as cardiovascular disorders.

In short, the N-Hcy-hTrx1 appears to have three major functional consequences, each contributing to potential pathological effects. (i) Impaired Redox Activity. N-homocysteinylation at Lys36, near the active-site Cys residues (Cys32/Cys35), may sterically or electrostatically hinder the interaction between hTrx1 and thioredoxin reductase (TrxR) or substrates. This disruption could compromise hTrx1's antioxidant and redox-regulatory functions, leading to oxidative stress and impaired cellular signaling. (ii) Aggregation-Prone Hydrophobic Surfaces. N-Hcy-hTrx1(II)/(III)) forms hydrophobic patches on its surface, promoting protein aggregation. These aggregates may act as seeds for further misfolding or amyloid formation, contributing to protein deposition diseases. (iii) Enhanced Cytotoxicity of Amyloid Fibrils. N-Hcy-hTrx1(II)/(III) forms amyloid fibrils that are ~667 times more toxic to cells than HCTL alone. These fibrils may circulate systemically and disrupt organ function, potentially contributing to endothelial damage and atherosclerosis. Thus, the systemic presence of these toxic species could explain the multi-organ damage seen in hyperhomocysteinemia.

In conclusion, our findings identify extracellular hTrx1 as the primary target of HCTL cytotoxicity, shifting the focus from its intracellular counterpart. This discovery clarifies a key mechanism of HCTL-induced cell damage and provides a new perspective on hyperhomocysteinemia-related pathogenesis. Future research should develop interventions targeting this extracellular pathway to mitigate HCTL-dependent cellular injury.

Experimental procedures

Materials

DTT, DL-HCTL, bovine pancreatic insulin, 8-Anilino-1-naphthalenesulfonic acid (ANS), thioflavin T (ThT), MTT, DTNB, PMSF, and NADPH were purchased from

Sigma-Aldrich Co. (St. Louis, MO, USA). Recombinant His-tag hTrx1 and calf-liver TrxR1 were prepared following the method described previously [27,28]. The anti-hTrx1 monoclonal antibody was purchased from Santa Cruz Biotechnology, Inc. (Santa Cruz, CA, USA). The anti-Hcy polyclonal antibody was purchased from Abcam (Cambridge, UK). The human umbilical vein cell line (EA. hy926) was obtained from the American Type Culture Collection (ATCC). Human sera were the remaining samples from a previous study [21].

Preparation of N-Hcy-hTrx1

Since stored hTrx1 can form intermolecular disulfide bonds, the protein was incubated with 30 mM DTT for 30 minutes to reduce these bonds, followed by dialysis against 50 mM Tris-HCl, pH 7.5, containing 1 mM EDTA (TE buffer). The freshly treated hTrx1 (30 μ M) was then incubated with a 10-fold, 50-fold, or 100-fold molar excess of HCTL per Lys residue at 37°C for 24 hours, followed by dialysis to remove any unbound HCTL. The resulting proteins were referred to as N-Hcy-hTrx1(I), N-Hcy-hTrx1(II), respectively.

The HCTL/hTrx1 ratios were established based on literature reports indicating that the serum level of tHcy in healthy adults ranges from 5 to 10 μM , while in mild cases it may range from 15 to 20 μM , and in hyperhomocysteinemia, it can rise up to 500 μM [29,30]. Under physiological conditions, HCTL is mostly neutral, freely diffuses through cell membranes, and is mostly present in extracellular media [7,30]. HCTL represents 0 to 0.28% of plasma tHcy, with an average of 0.023 \pm 0.05% (31). In cases of extreme intercellular Hcy elevation, HCTL levels can reach up to 60% of the metabolized Hcy [6]. On the other hand, the mean level of serum hTrx1 in South Korean women is approximately 0.45 nM [32], while in Chinese healthy adults it is about 0.84 to 1.2 nM [3,21], and in patients with acute exacerbation of asthma, it reaches approximately 3.24 nM [33].

Analyzing the serum Hcy-hTrx1 complex and the effect of extracellular HCTL on cellular hTrx1.

To determine if the Hcy-hTrx1 complex is present in human serum, a serum sample containing 750 μ g of total protein was immunoprecipitated with an anti-Hcy polyclonal antibody. Subsequently, the antibody was collected using protein A+G agarose beads. The obtained immune complexes were washed five times with cold PBS. The presence of Hcy-hTrx1 was then detected through Western blot analysis using an anti-hTrx1 monoclonal antibody. To analyze the effect of extracellular HCTL on the localization of cellular hTrx1 and Hcy using immunofluorescence, cells were cultured on cover glass (NEST, China) within a 24-well plate and treated with varying concentrations of HCTL for 24 hours.



Subsequently, the cells were fixed in 4% paraformaldehyde (PFA) for 20 minutes, permeabilized with 0.1% Triton X-100 for 30 minutes and blocked with 3% BSA for 2 hours at room temperature. The cells were then incubated with antihTrx1 monoclonal antibody or anti-Hey polyclonal antibody, both diluted 1:100 (v/v) in 3% BSA, overnight. Following this, they were treated with FITC- or TRITC-conjugated secondary antibody (ZSGB-BIO, China), also diluted 1:100 (v/v) in 3% BSA, for 2 hours at room temperature. Finally, the cells were fixed with ProLongTM Gold antifade reagent containing 4',6-diamidino-2-phenylindole (DAPI, used as a nuclear counterstain) (Invitrogen, USA) and detected using a LEICA DM 6000B microscope (Leica Microsystems, Wetzlar, Germany). To analyze the hTrx1 mRNA level, the quantitative real-time PCR technique was used following the method described in [34]. To test the level of Hcy-hTrx1 complex, an aliquot (containing 1 mg of protein) from the cell extracts was incubated with anti-hTrx1 monoclonal antibody overnight at 4°C. Subsequently, the complexes were isolated using Protein A+G agarose beads for 2 hours at 4°C, followed by five washes with cold PBS. The levels of Hcy-hTrx1 complex from Co-IP samples and the expression of hTrx1 from cell extracts were analyzed using Western blot with anti-Hcy polyclonal antibody and anti-hTrx1 monoclonal antibody, respectively. The Trx activity in cell extracts was determined in 96-well plates using a super-insulin assay [35].

Analyzing the effect of extracellular HCTL on the cellular hTrx1's thiol states, ROS levels, and cell viability.

The thiol states of cellular Trx1 were detected using methods previously described [36]. Aliquots (24.5 µg protein) from the cell extracts were separated using urea-PAGE gel and then transferred to a PVDF membrane. The membrane was probed with an anti-hTrx1 monoclonal antibody, followed by a biotinylated secondary antibody and a Streptavidin-ALP anti-biotin tertiary antibody (ZSGB-BIO, Beijing, China). The proteins were then visualized using a 5-Bromo-4-chloro-3-indolyl-phosphate/Nitro Blue Tetrazolium (BCIP/NBT) solution (Amresco, WA, USA). Cellular ROS levels were measured using the method described in [34]. The assay of cell viability was conducted as follows. EA. hy926 cells, serving as a model for vascular endothelial cells, were cultured in DMEM medium (Gibco, USA) supplemented with 10% fetal bovine serum (FBS) within a humidified incubator under a 5% CO, atmosphere at 37°C. For the MTT assay, the cells were grown in 96well microplates until they reached 70 to 80% confluence. The medium was then replaced with DMEM supplemented with 5% FBS, followed by the addition of 1.5 μM of various forms of N-Hcy-hTrx1 or 0 to 5 mM HCTL, respectively. After 24 hours, a 150-µl aliquot of MTT solution (0.5 mg/ml) was added to each well and incubated at 37°C for 4 hours.

The MTT-formazan product was dissolved in DMSO. The absorbance at 492 nm was then measured. For the CCK-8 assay, Cell Counting Kit-8 (DOJINDO, Japan) was utilized. Following the manufacturer's protocol, a 10-µl aliquot of CCK-8 was added to each well, and the plate was incubated for 2 hours before measuring the absorbance at 450 nm.

Analyzing the general properties of N-Hcy-hTrx1

To identify HCTL-targeted Lys residues in hTrx1 using Mass Spectrometry, N-Hcy-hTrx1 (III) was further purified via SDS-PAGE. Subsequently, the protein band was excised from the gel and each gel slice was diced into small pieces. The resulting sample was then reduced with DTT and modified with IAM, followed by in-gel trypsin digestion. Finally, the extracted peptides were analyzed by LC-ESI-MS/MS, utilizing a Biobasic-18 column (0.18×150 mm) (Surveyor HPLC system, Thermo, Thermo Inc.), coupled with an ion trap mass spectrometer (LCQ DECA Xp plus; ThermoFinnigan, Inc., USA). This work was conducted in the State Key Laboratory of Membrane Biology, Institute of Zoology, Chinese Academy of Sciences. The activity of purified hTrx1 or N-Hcy-hTrx1 was measured using insulin reduction assay [37]. To analyze N-homocysteinylationinduced aggregation, solutions of hTrx1 and N-Hcy-hTrx1 (III) were centrifuged separately. The hTrx1 solution showed no precipitate, whereas the N-Hcy-hTrx1 (III) solution exhibited a precipitate. The precipitate was then resuspended in TE buffer for analysis using 12% SDS-PAGE. To determine whether N-homocysteinylation might alter the sensitivity of hTrx1 to Proteinase K, hTrx1 and N-Hcy-hTrx1(III) (both at 35 μM) were incubated with 0.05 mg/ml Proteinase K (Beyotime, China) for varying durations (0, 10, 20, 40 minutes) at 37°C. The resulting samples were then separated using 12% SDS-PAGE, and the protein bands were visualized with Coomassie Brilliant Blue R-250. To test for the presence of the anti-N-Hcy-hTrx1 autoantibody in human serum, hTrx1 and N-Hcy-hTrx1(I) were separately spotted onto a nitrocellulose membrane and incubated overnight with a 1:10 dilution of human serum, serving as the primary antibody. A 1:1000 dilution of alkaline phosphatase- conjugated goat anti-human IgG was utilized as the secondary antibody, with BCIP/NBT serving as the substrate for the alkaline phosphatase.

Analyzing the effect of N-homocysteinylation on hTrx1 structure

To determine the changes in secondary structure, circular dichroism (CD) spectra of hTrx1 and N- Hcy-hTrx1 (0.05 mg/ml) were detected using a J-815 CD spectrometer (JASCO, Japan). Measurements were performed between 190 nm and 250 nm with a scan rate of 200 nm/min. Data were calibrated by subtracting the buffer ellipticity and were expressed in units of deg·cm²·dmol⁻¹/residue (θ).



To observe structural changes specifically around the active site, the fluorescence intensities of Trp, Tyr, and ANS were determined using a HITACHI F-4700 fluorescence spectrophotometer (HITACHI, Japan). In the intrinsic (Trp and Tyr) fluorescence study, aliquots of 2.4 µM hTrx1 or N-Hcy-hTrx1(I)/(III) were analyzed using an excitation wavelength of 290 nm and emission spectra ranging from 280 nm to 500 nm, with a slit width of 5 nm. For ANS experiments (to reveal the hydrophobic sites), aliquots of 5 μM hTrx1 or N-Hcy-hTrx1(I)/(III) were incubated with a 20-fold molar excess of freshly prepared ANS (dissolved in N, N-Dimethylformamide) at 37°C for 60 minutes in the dark. The excitation was set at 365 nm, and the emission spectra were recorded between 400 nm and 600 nm. To monitor the formation of amyloid fibrils, ThT fluorescence was measured. Aliquots of 5 μM hTrx1 or N-Hcy-hTrx1(I)/ (III) were incubated with freshly prepared ThT (1:10) for 5 minutes. Spectra of ThT fluorescence were acquired using an excitation wavelength of 435 nm and emission spectra between 450 nm and 600 nm. Alternatively, freshly prepared ThT was incubated with 24 µM hTrx1 or N-Hcy-hTrx1(II) at a molar ratio of 20:1. The resulting samples were analyzed with a fluorescent microscope (LEICA DM 6000B) using an excitation filter of 340-380 nm and an emission range of 450-490 nm.

To observe changes in the molecular shape of N-HcyhTrx1, a fluorescence microscope, a differential interference contrast (DIC) microscope, and a transmission electron microscopy (TEM) were used. For the analysis under the microscope, a freshly prepared solution of ThT was mixed with 24 μM hTrx1 or N-Hcy-hTrx1(II) at a molar ratio of 20:1 and incubated at room temperature for 5 minutes. A 5-µl aliquot of this incubation mixture was placed on a glass slide. Their fluorescent and DIC images were taken using a Leica DM 6000B fluorescent microscope via DIC or FLUO modes. For TEM analysis, carbon-coated copper grids (200-mesh) were first hydrophilized using a Leica EM ACE200 glow discharge for 30 seconds at 14 mA. hTrx1 and N-Hcy-hTrx1(II) were both diluted to a concentration of 5 µM. A 5-µl sample of each was then spotted onto the grid and allowed to incubate for 1 minute. The grids were subsequently washed twice in 2% uranyl acetate before undergoing negative staining with the same solution for 1 minute. The samples were examined under a Tecnai G2 F20 TWIN TMP (FEI, USA) transmission electron microscope operated at 200 kV.

Statistical analysis

Intergroup comparisons were performed using one-way ANOVA with Tukey's post-hoc test. A p-value < 0.05 was considered statistically significant, while p < 0.01 was regarded as highly significant. All analyses were performed using GraphPad Prism 5.0.

Acknowledgements

We sincerely thank Professor Yujian He from the School of Chemical Sciences, University of Chinese Academy of Sciences, for his generous assistance and for providing access to the J-815 CD spectrometer. We are also grateful to the State Key Laboratory of Membrane Biology at the Institute of Zoology, Chinese Academy of Sciences, for their technical support in transmission electron microscopy and mass spectrometry.

Author contributions

Ping Liu: Experimental design, execution, data analysis and interpretation, and manuscript preparation. Liangwei Zhong: Supervision, manuscript revision, and funding acquisition.

Funding information

This work was supported by the National Natural Science Foundation of China (Grant Nos. 30970629 and 31170764) and the Ministry of Science and Technology of the People's Republic of China (2009ZX09103-432).

Conflict of interest

The authors declare no competing interests, financial or otherwise, related to this work.

Reference

- 1. Luhmann D, Schramm S, Raspe, H. The role of Homocysteine as a predictor for coronary heart disease. GMS Health Technol Assess 3 (2007).
- Wu Y, Yang L, Zhong L. Decreased serum levels of thioredoxin in patients with coronary artery disease plus hyperhomocysteinemia is strongly associated with the disease severity. Atherosclerosis 212 (2010): 351-355.
- 3. Li J, Wang P, Xiao L, et al. Serum thioredoxin activity: a promising biomarker for assessment of coronary stenosis severity in patients with coronary artery disease. Science Bulletin 62 (2017): 752-754.
- Mudd S H, Finkelstein, J D, Refsum, et al. Homocysteine and its disulfide derivatives: a suggested consensus terminology. Arterioscler. Thromb. Vasc. Biol. 20 (2000): 1704-1706.
- Jakubowski H, Głowacki, R. Chemical biology of homocysteine thiolactone and related metabolites. Adv. Clin. Chem. 55 (2011): 81-103.
- 6. Jakubowski H. Homocysteine thiolactone: metabolic origin and protein homocysteinylation in humans. J. Nutr. 130 (2000): 377-381.



- Jakubowski H. The determination of homocysteinethiolactone in biological samples. Anal. Biochem 308 (2002): 112-119.
- 8. Jakubowski H. Homocysteine Modification in Protein Structure/Function and Human Disease. Physiol. Rev 99 (2019): 555-604.
- Sharma GS, Kumar T, Dar TA, et al. Protein N-homocysteinylation: From cellular toxicity to neurodegeneration. Biochim Biophys Acta 1850 (2015): 2239-2245.
- Jakubowski H. Pathophysiological consequences of homocysteine excess. J. Nutr 136 (2006): 1741- 1749.
- 11. Paoli P, Sbrana F, Tiribilli B, et al. Protein N-homocysteinylation induces the formation of toxic amyloid-like protofibrils. J. Mol. Biol 400 (2010): 889-907.
- Khodadadi S, Riazi G H, Ahmadian S, et al. Effect of N-homocysteinylation on physicochemical and cytotoxic properties of amyloid beta-peptide. FEBS Lett 586 (2012): 127-131.
- 13. Jakubowski H, Zhang L, Bardeguez A, et al. Homocysteine thiolactone and protein homocysteinylation in human endothelial cells: implications for atherosclerosis. Circ. Res 87 (2000): 45-51.
- Jakubowski H. Protein N-homocysteinylation: implications for atherosclerosis. Biomed. Pharmacother 55 (2001): 443-447.
- Collet J F, Messens J. Structure, function, and mechanism of thioredoxin proteins. Antioxid. Redox Signal. 13 (2010): 1205-1216.
- Arner E S, and Holmgren, A. Physiological functions of thioredoxin and thioredoxin reductase. Eur. J. Biochem 267 (2000): 6102-6109.
- Yamawaki H, Haendeler J, Berk B C. Thioredoxin: a key regulator of cardiovascular homeostasis. Circ. Res. 93 (2003): 1029-1033.
- 18. Hirota K, Murata M, Sachi Y, et al. Distinct roles of thioredoxin in the cytoplasm and in the nucleus. A two-step mechanism of redox regulation of transcription factor NF-kappaB. J. Biol. Chem 274 (1999): 27891-27897.
- 19. Floen M J, Forred B J, Bloom E J, et al. Thioredoxin-1 redox signaling regulates cell survival in response to hyperoxia. Free Radic. Biol. Med 75 (2014): 167-177.
- 20. Hanschmann E M, Petry S F, Eitner S, et al. Paracrine regulation and improvement of β-cell function by thioredoxin. Redox Biol 34 (2020): 101-570.

- 21. Bai Y, Liu J, Yang L, et al. New insights into serum/extracellular thioredoxin in regulating hepatic insulin receptor activation. Biochim Biophys Acta Gen Subj 1864 (2020): 129-630.
- Billiet L, Furman C, Larigauderie G, et al. Extracellular human thioredoxin-1 inhibits lipopolysaccharide-induced interleukin-1beta expression in human monocyte-derived macrophages. J. Biol Chem 280 (2005): 40310-40318.
- 23. Nakamura H. Extracellular functions of thioredoxin. Novartis Found. Symp 291 (2008): 184-192.
- 24. Hashemy S I, Holmgren A. Regulation of the catalytic activity and structure of human thioredoxin 1 via oxidation and S-nitrosylation of cysteine residues. J. Biol. Chem 283 (2008): 21890-21898.
- 25. Casagrande S, Bonetto V, Fratelli M, et al. Glutathionylation of human thioredoxin: a possible crosstalk between the glutathione and thioredoxin systems. Proc. Natl. Acad. Sci. U. S. A 99 (2002): 9745-9749.
- 26. Xu Z, Zhong L. New insights into the posttranslational regulation of human cytosolic thioredoxin by S-palmitoylation. Biochem Biophys Res Commun 31 (2015): 00598-00597.
- 27. Ungerstedt J, Du Y, Zhang H, et al. In vivo redox state of human thioredoxin and redox shift by the histone deacetylase inhibitor suberoylanilide hydroxamic acid (SAHA). Free Radic. Biol. Med 53 (2012): 2002-2007.
- 28. Du Y, Zhang H, Zhang X, et al. Thioredoxin 1 is inactivated due to oxidation induced by peroxiredoxin under oxidative stress and reactivated by the glutaredoxin system. J. Biol. Chem 288 (2013): 32241-32247.
- 29. Undas A, Perla J, Lacinski M, et al. Autoantibodies against N-homocysteinylated proteins in humans: implications for atherosclerosis. Stroke 35 (2004): 1299-1304.
- 30. Hall G, and Emsley J. Structure of human thioredoxin exhibits a large conformational change. Protein Sci 19 (2010): 1807-1811.
- 31. Reutimann H, Straub B, Luisi P L, et al. A conformational study of thioredoxin and its tryptic fragments. The Journal of biological chemistry 256 (1981): 6796-6803.
- 32. Teale F W, Weber G. Ultraviolet fluorescence of the aromatic amino acids. Biochem. J 65 (1957): 476-482.
- 33. Holmgren A. Tryptophan fluorescence study of conformational transitions of the oxidized and reduced form of thioredoxin. J. Biol. Chem. 247 (1972): 1992-1998.
- 34. Weichsel A, Gasdaska J R, Powis G, et al. Crystal structures of reduced, oxidized, and mutated human



- thioredoxins: evidence for a regulatory homodimer. Structure 4 (1996): 735-751.
- 35. Hawe A, Sutter, M, Jiskoot. Extrinsic fluorescent dyes as tools for protein characterization. Pharm. Res 25 (2008): 1487-1499.
- 36. LeVine H. Thioflavine T interaction with synthetic Alzheimer's disease beta-amyloid peptides: detection of amyloid aggregation in solution. Protein Sci. 2 (1993): 404-410.
- 37. Xiao Z X, Miller J S, Zheng S G. An updated advance of autoantibodies in autoimmune diseases. Autoimmun. Rev. 20 (2021): 102743.
- 38. Conrad N, Verbeke G, Molenberghs G, et al. Autoimmune diseases and cardiovascular risk: a population-based study on 19 autoimmune diseases and 12 cardiovascular diseases in 22 million individuals in the UK. Lancet 400 (2022): 733-743.
- 39. Silla Y, Varshney S, Ray A, et al. Hydrolysis of homocysteine thiolactone results in the formation of Protein-Cys-S-S-homocysteinylation. Proteins 87 (2019): 625-634.
- 40. Nishinaka Y, Masutani H, Nakamura H, et al. Regulatory roles of thioredoxin in oxidative stress-induced cellular responses. Redox Rep 6 (2001): 289-295.
- 41. Zimny J, Sikora M, Guranowski A, et al. Protective

- mechanisms against homocysteine toxicity: the role of bleomycin hydrolase. J. Biol. Chem 281 (2006): 22485-22492.
- 42. Oblong J E, Berggren M, Gasdaska P Y, et al. Site-directed mutagenesis of Lys36 in human thioredoxin: the highly conserved residue affects reduction rates and growth stimulation but is not essential for the redox protein's biochemical or biological properties. Biochemistry 34 (1995): 3319-3324.
- 43. Sharma G S, Kumar T, Singh L R. N-homocysteinylation induces different structural and functional consequences on acidic and basic proteins. PLoS One 9 (2014): e116386.
- 44. Manning M, Colón W. Structural basis of protein kinetic stability: resistance to sodium dodecyl sulfate suggests a central role for rigidity and a bias toward beta-sheet structure. Biochemistry 43 (2014): 11248-11254.
- 45. Marshall K E, Marchante R, Xue W F, et al. The relationship between amyloid structure and cytotoxicity. Prion 8 (2014): 192-196.
- 46. Xue C, Lin T Y, Chang D, et al. Thioflavin T as an amyloid dye: fibril quantification, optimal concentration and effect on aggregation. R Soc Open Sci 4 (2017): 160696.
- 47. Arad E, Green H, Jelinek R, et al. Revisiting thioflavin T (ThT) fluorescence as a marker of protein fibrillation The prominent role of electrostatic interactions. J Colloid Interface Sci 573 (2020): 87-95.

